Tuesday, October 14, 2003
Morning Session II
GEOLOGY OF THE MARTIAN SOUTH POLAR LAYERED DEPOSITS
10:30 a.m. Victoria Room

Head J. W. * Ghatan G. J. Marchant D. [INVITED]
Extensive Hesperian-aged South Circumpolar Ice Sheet on Mars: Dorsa Argentea Formation Synthesis **[#8067]**

Herkenhoff K. E. * Soderblom L. A. Kirk R. L. [INVITED]
Stratigraphy and Structure of the South Polar Layered Deposits on Mars **[#8030]**

Thomas P. C. *
The South Polar Residual Cap of Mars: Layers, Erosion, and Stratigraphy **[#8047]**

Byrne S. * Ingersoll A. P. Pathare A. V. Jiron F. S.
Climactic History from South Polar Residual Cap Geomorphology **[#8037]**

12:00 – 1:30 p.m. LUNCH

EXTENSIVE HESPERIAN-AGED SOUTH CIRCUMPOLAR ICE SHEET ON MARS: DORSA ARGENTEA FORMATION SYNTHESIS:

James W. Head[1], Gil J. Ghatan[1] and David Marchant[2], [1]Dept. Geol. Sci, Brown Univ., Providence, RI 02912 USA, [2]Dept. Earth Sciences, Boston Univ., Boston, MA 02215 USA, james_head@brown.edu

Introduction and background: The nature of the climate in early Mars history, and whether pluvial conditions prevailed [e.g., 1] during the Noachian Period (~4.6-3.7 Ga) [2], or if an ocean existed then and/or during the Hesperian Period (~3.7-3.0 Ga) [3], are matters of major debate and investigation. The Dorsa Argentea Formation [4] (DAF) is a south circumplolar deposit of Hesperian age [2] and thus may record the aftermath of Noachian-aged climate and volatile evolution. Here we outline a synthesis of the characteristics of the DAF, and show that these are consistent with the presence of a major water-ice-rich circumpolar deposit during the Hesperian, and its partial melting, sublimation and retreat. We outline interpretations for the source and fate of these volatiles and their significance to polar and hydrological processes and history.

The Dorsa Argentea Formation: Underlying the present Amazonian-aged polar cap (Api, residual ice and Apl, layered terrain) lies the Hesperian-aged Dorsa Argentea Formation, Hd, and related units [4] (Figure 1) (here collectively called the DAF). This deposit covers a surface area that could be as large as 2.94 x 10^6 km^2 (about 2% of the surface of Mars), over twice the area of the present Amazonian-aged deposits. Originally interpreted as largely volcanic in origin [4], this deposit has been reinterpreted on the basis of new MGS data as a volatile-rich ice-sheet-like unit that underwent melting and retreat [5] or, alternatively, a deposit caused by release and emplacement of subsurface volatiles and debris [6]. Here we synthesize the evidence for the DAF and related units representing an extensive south circumpolar glacial-like deposit that underwent significant melting, sublimation and retreat [5].

Sinuous Channels Along the Eastern DAF Margin: Along the eastern margin of the continuous deposit of the DAF (Figure 1; 1) are located a series of sinuous channels that lead away from the margin of the deposit and enter nearby craters, exiting them from downslope margins, crossing intercrater terrain and entering other craters [7]. The channels connecting these craters provide evidence for extensive crater flooding, ponding (minimum volumes of ~10^{12} m^3), overtopping, downcutting, and continuous drainage of material through a series of craters and into the Prometheus Basin near the edge of the current polar cap. Topogrpahy data show that water filled some craters to depths of at least 200 m and possibly as much as 600 m. Water exiting from the edge drained over a lateral distance of ~600 km and a vertical height of ~800 m. These data provide evidence for the water-rich nature of the DAF, its subsequent melting and collapse, and the overland drainage of its meltwater effluent [7].

Concentric Ridges: Nearby these marginal channels but inward of the DAF margin (Figure 1, 2) lies a series of arcuate ridges that are convex-outward from the DAF margin. These have been interpreted to be push moraines derived from bulldozing of ice and sediment at the margins of the DAF [8].

Sisyphi Lobe and Broad Depression: One of two major lobes of the DAF is the Sisyphi Lobe that extends out from the south pole toward 0° (Figure 1). Largely surrounded by Noachian cratered terrain, the deposit in this area is shown by MOLA data to be a topographic low [9], and smooth at small scales, but containing a large-scale pitted texture and a number of unusual mountains.

Unusual Mountains: Located within the Sisyphi Lobe are a number of isolated mountains with average separation distances of ~175 km (Figure 1; 3); these are typically 30-40 km in diameter and ~1-1.5 km high, with their bases falling near an elevation of ~1200 m. The unusual shapes of these mountains as well as the alignment of many, and the sinuous channels emanating from the base of several, has led to the interpretation [10] that they are of volcanic origin, with their unusual morphology and morphometry being accounted for by their eruption under an ice-sheet. Assessment of edifice morphometry led to the conclusion that the overlying ice sheet had a minimum thickness of ~1.4 km [10].

Cavi Sisyphi: Located within the Sisyphi Lobe are a series of irregular and elongate depressions that are typically about 500 m deep and have relatively steep marginal slopes (~11°) (Figure 1; 4). Within several of these are sinuous ridges that have been interpreted to be eskers and are oriented in directions consistent with regional drainage from regions within the DAF that appear to have undergone melting (likely related to the features interpreted as subglacial volcanoes) and drainage toward the margins of the DAF where large channels emerge and wind toward the floor of Argyre [11].

Angusti Lobe: Oriented radially from the south pole toward 70° W is a broad lobe of positive topography which we describe as the Angusti Lobe (Figure 1).

Cavi Angusti: Within the Angusti Lobe lie Cavi Angusti (Figure 1; 5), a series of basins similar to Cavi Sisyphi in surface area and wall steepness, but differeing in several important ways. These basins are typically deeper (~1000 m) and contain centrally located mountains or ridges, which have been interpreted to be volcanic edifices [12]. The terraced interiors and central mountains of many cavi have been interpreted to mean that the basins formed as a result of magmatic intrusion and extrusions causing heating and melting of a water-rich substrate (the overlying DAF) and drainage of the liquid water. Meltwater from basin formation appears to have drained laterally and may also have reentered the subsurface groundwater system [12].

Dorsa Argentea: A series of sinuous and overlapping ridges extend for several hundreds of km from the interior of the DAF toward the margins (Figure 1; 6). A range of different interpretations have been offered in the past [5] but recently terrestrial analogs and topography data have been used to develop detailed criteria for the recongnition of eskers on Mars [13]. Application of these criteria has strengthened the interpretation that these ridges are eskers and that they represent the drainage of meltwater products from the interior of the DAF toward the margins, out into an adjacent lowlying region interpreted to be a lake [14].

Lowlands Around Schmidt Crater: Adjacent to the Angusti Lobe is a low-lying smooth area (Figure 1; 7) interpreted to be a region in which meltwater from the central DAF was delivered and which collected before ultimately draining through a channel in the surrounding topography and down into the Argyre Basin. Informally called Lake Schmidt, this region covers an area of ~270,000 km^2, five times the size of Lake Michigan and may have been in excess of 300 m deep [14]. Also observed is a series of pits in a narrow zone located along the boundary between the Angusti lobe and the adjacent lowlands; this has been interpreted to be a contact zone between the ice sheet and the lake, in which the pits are comparable to kettle holes formed due to melting of residual ice blocks [15].

Pedestal Craters: Craters with extensive elevated ejecta deposits occur within the DAF with the most prominent one (Figure 1; 8) characterized by marginal ~500 m high scarps [5], suggesting that material removed from below this armoring deposit was at least 500 m thick.

Mountains near South Crater: A series of distinctive mountain peaks occur near South crater (Figure 1; 9) and their morphology suggests that their lower portions were buried by the DAF but that their upper portions were surrounded by the DAF. On the basis of their morphology and unusual structure, we have interpreted these to be nunataks, mountains which rise above surrounding ice sheets.

Hr relationships: Located along the eastern edge of the Sisyphi Lobe (Figure 1; 10), and defining the margin of the DAF is an extensive scarp between the DAF and Hr (ridged plains interpreted to be of volcanic origin). This unusual scarp faces inward toward the DAF and is interpreted to have formed by the emplacement of Hr lavas from sources in Malea Planum up against the DAF, forming a constructional ridge against the ice sheet. Subsequent to the decay of the ice sheet the scarp remains and is now facing inward toward the DAF. The presence of this scarp may help to explain why much of the meltwater appears to have drained into the Prometheus and Argyre Basins, and not out into Hellas.

Channels Marginal to the DAF: Inspection of the DAF along the western margins of the Sisyphi Lobe, as well as along the eastern margins of the Angusti Lobe, reveals the presence of channels that are arrayed radially away from the deposit (Figure 1, white lines). These several large channels begin at and near the margins of the DAF; some can be traced back into the deposit and are continuous with esker-like ridges and elongate cavi in the DAF [16]. These channels lead from the DAF margins northward, draining downslope for distances from 1000-1600 km onto the floor of the Argyre Basin, some 3.5-4.0 km below their origins. The channels do not exhibit tributaries and are sometimes discontinous in flat regions where ponding may have taken place. Their characteristics suggest that a significant portion of the DAF meltwater entered a surface distribution system that transported it to the floor of Argyre [5].

Synthesis: These characteristics of the DAF and adjacent deposits lead us to the interpretation that the unit represents the remnants of a major south circumpolar ice-rich deposit that existed in the Hesperian and that underwent significant melting, sublimation and retreat. Estimates of the present deposit thickness, and the amount of material thought to have been removed suggest that the original volume could have been as much as 5.9 x 10^6 km^3, equivalent to a global layer of water ~20 m deep if the deposit consisted of 50% volatiles. Positive evidence is seen for bottom-up melting (volcanic eruptions); top-down melting may also have occurred. Some of the water from this melting drained laterally overland, but a significant portion may well have entered the groundwater system, potentially recharging the global aquifer [3]. A portion of the volatiles are predicted to have remained in the deposit, representing a net removal from the atmosphere and from the active hydrologic system. Today the DAF forms an accessible record of aqueous conditions and possible biological environments dating from early Mars history.

References: 1) R. Craddock and A. Howard, JGR, 10.1029/2001JE001505, 2002; 2) W. Hartmann and G. Neukum, Space Sci. Rev., 96, 165, 2001; 3) S. Clifford and T. Parker, Icarus, 154, 40, 2001; 4) K. Tanaka and D. Scott, USGS Map 1802-C, 1987; 5) J. Head and S. Pratt, JGR, 106, 12275, 2001; 6) K. Tanaka and E. Kolb, Icarus, 154, 3, 2001; 7) S. Milkovich et al., JGR, 10.1029/2001JE001802, 2002;.8) S. Milkovich and J. Head, Microsymposium 24, 2001;. 9) J. Head and G. Ghatan, LPSC 32, #1062, 2001; 10) G. Ghatan and J. Head, JGR, 10.1029/2001JE001519, 2002; 11) G. Ghatan and J. Head, LPSC 34, #1129, 2003; 12) G. Ghatan et al., JGR, 10.1029/2002JE001972, 2003; 13) J. Head and B. Hallet, LPSC 32, #1366, #1373, 2001; 14) J. Head and S. Pratt, LPSC 32, #1159, 2001; 15) J. Dickson and J. Head, LPSC 34, #1185, 2003; 16) G. Ghatan and J. Head, 6th Mars Conf., #3034.

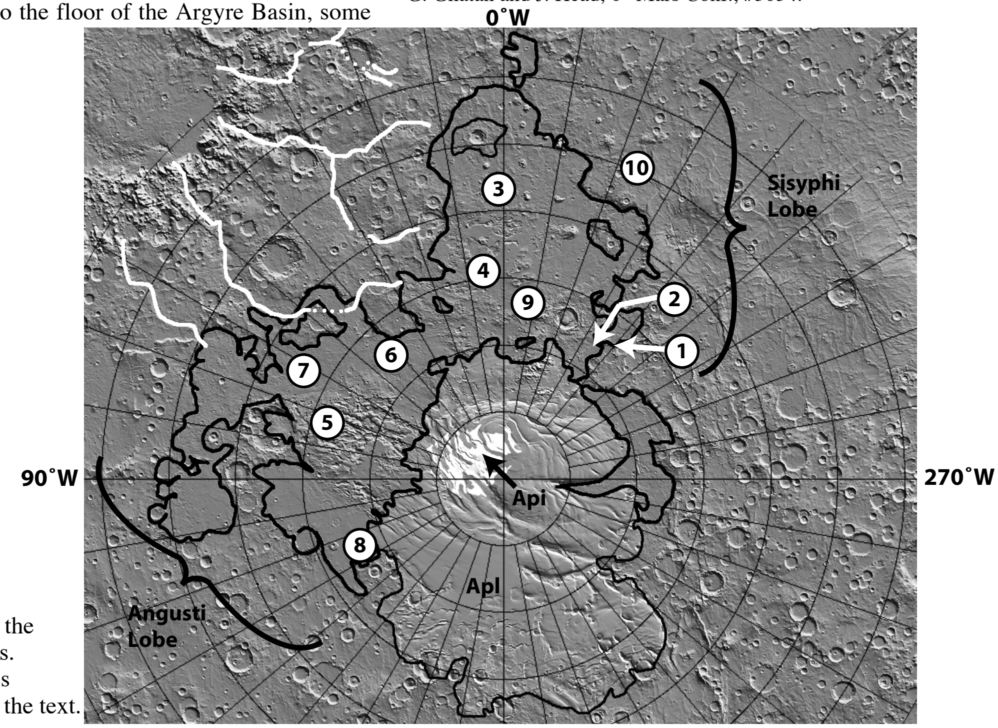

Figure 1. Distribution of the DAF and related deposits. Numbers refer to features and regions described in the text.

STRATIGRAPHY AND STRUCTURE OF THE SOUTH POLAR LAYERED DEPOSITS ON MARS.

K. E. Herkenhoff, L. A. Soderblom and R. L. Kirk, U. S. Geological Survey Astrogeology Team, 2255 N. Gemini Dr., Flagstaff, AZ 86001 (kherkenhoff@usgs.gov).

Introduction: The martian polar layered deposits (PLD) are probably the best source of information about the recent climate history of Mars [1-7], but their origin and the mechanisms of accumulation are still a mystery [8]. The polar layers are sedimentary deposits that most planetary scientists believe are composed of water ice and varying amounts of wind-blown dust [2-4], but their composition is poorly constrained [9]. Because climate changes are likely recorded as variations in composition or deposition/erosion rates between layers, the detailed stratigraphy of the PLD is of great interest. Layer thicknesses of ~10 to 50 m were observed in Viking Orbiter images of the north PLD by Blasius *et al*. [10], and Mars Orbiter Camera (MOC) images resolve layers with similar or lesser thicknesses in both polar regions [11]. In order to accurately determine the thickness of layers and interpret PLD stratigraphy and structure, the topography of exposures must be known. Previous studies have identified deformation in the PLD similar to that observed in terrestrial glaciers [12-14], but lack of detailed topography has hindered structural interpretations. Here we describe results of our continuing study to evaluate the topography, structure, and stratigraphy of the south PLD using photoclinometry on MOC images.

Approach: Because the south PLD surface is typically rough (Fig. 1), we used a 2-dimensional photoclinometric technique [15] constrained using simultaneously-acquired MOLA data. This technique is well suited to images taken at high latitudes when the surface was covered by seasonal frost and the solar elevation angle was low so that albedo variations and their effects are minimized and topographic modulation is emphasized (Fig. 1). The high density of MOLA data in the polar regions allows gridded topographic products to be generated at higher spatial resolution (~250 m/pixel) than is possible at lower latitudes. We introduce MOLA topography into the process in five ways [16]: 1) for planimetric control; 2) to precisely model surface and atmospheric reflectance/scattering; 3) to account for subtle variations in surface albedo; 4) as the starting solution for the photoclinometric model; 5) as the DEM base map on which the MOC NA high-resolution DEMs are mosaicked. A sample of the results of this approach is shown in Figure 2.

Results: The photoclinometric models show evidence for folding and faulting of the PLD. Figure 2 shows what appear to be folded beds between relatively planar layers. The planar layers are in some places truncated by the folded layers, either from above or below. These relations suggest that the folds are not simply the result of compression of the entire stack of PLD, although the layers at the bottom of the exposure in Figure 2 may have been folded in this way.


Figure 1. Part of MOC image m0402455 of apparent reverse faults in south PLD. Illumination from bottom left, 2.8 m/pixel.

For the wavy structures near the top of the section, deformation by faulting and/or flow is implied. If the folding was caused by ductile or fluid flow, erosion of the planar beds is required to produce the observed terminations. The flow process may have caused erosion of the adjacent layers, for example. The feature near the top of the section shown in Figure 2 is consistent with viscous flow down the current topographic slope. Alternatively, the truncations may have been caused by faulting along non-planar surfaces. For example, the wavy structure just above the green plane in Figure 1 may be a fault zone, formed by low-angle normal displacement with the slip vector trending approximately parallel to the present topographic gradient. Analysis of photoclinometric models of other PLD exposures will be discussed at the conference.

References: [1] Murray, B. C., *et al.* (1972). *Icarus* **17**, 328-345. [2] Cutts, J. A., *et al.* (1979). *J. Geophys. Res.* **84**, 2975-2994. [3] Squyres, S. W. (1979). *Icarus* **40**, 244-261. [4] Toon, O. B., *et al.* (1980). *Icarus* **44**, 552-607. [5] Carr, M. H. (1982). *Icarus* **50**, 129-139. [6] Howard, A. D., *et al.* (1982). *Icarus* **50**, 161-215. [7] Plaut, J. J., *et al.* (1988). *Icarus* **76**, 357-377. [8] Thomas, P., *et al.* (1992). In *Mars*, University of Arizona Press, Tucson, pp. 767-795. [9] Clifford, S. M. *et al.* (2000). *Icarus* **144**, 210-242. [10] Blasius, K. R., *et al.* (1982). *Icarus* **50**, 140-160. [11] M. C. Malin and Edgett, K. S. (2001). *J. Geophys. Res.* **106**, 23,429-23,570. [12] Kargel, J. S. (2001). *Eos, Trans. AGU.*, **82**, F724. [13] Brightwell, S. N., *et al.* (2003). *LPS XXXIV,* Abstract #2077. [14] Murray, B. C., *et al.* (2002). *Icarus* **154**, 80-97. [15] Kirk, R. L., *et al.* (2003). ISPRS Working Group IV/9 Workshop "Advances in Planetary Mapping 2003", Houston. [16] Soderblom, L. A. and Kirk, R. L. (2003). *LPS XXXIV,* Abstract #1730.

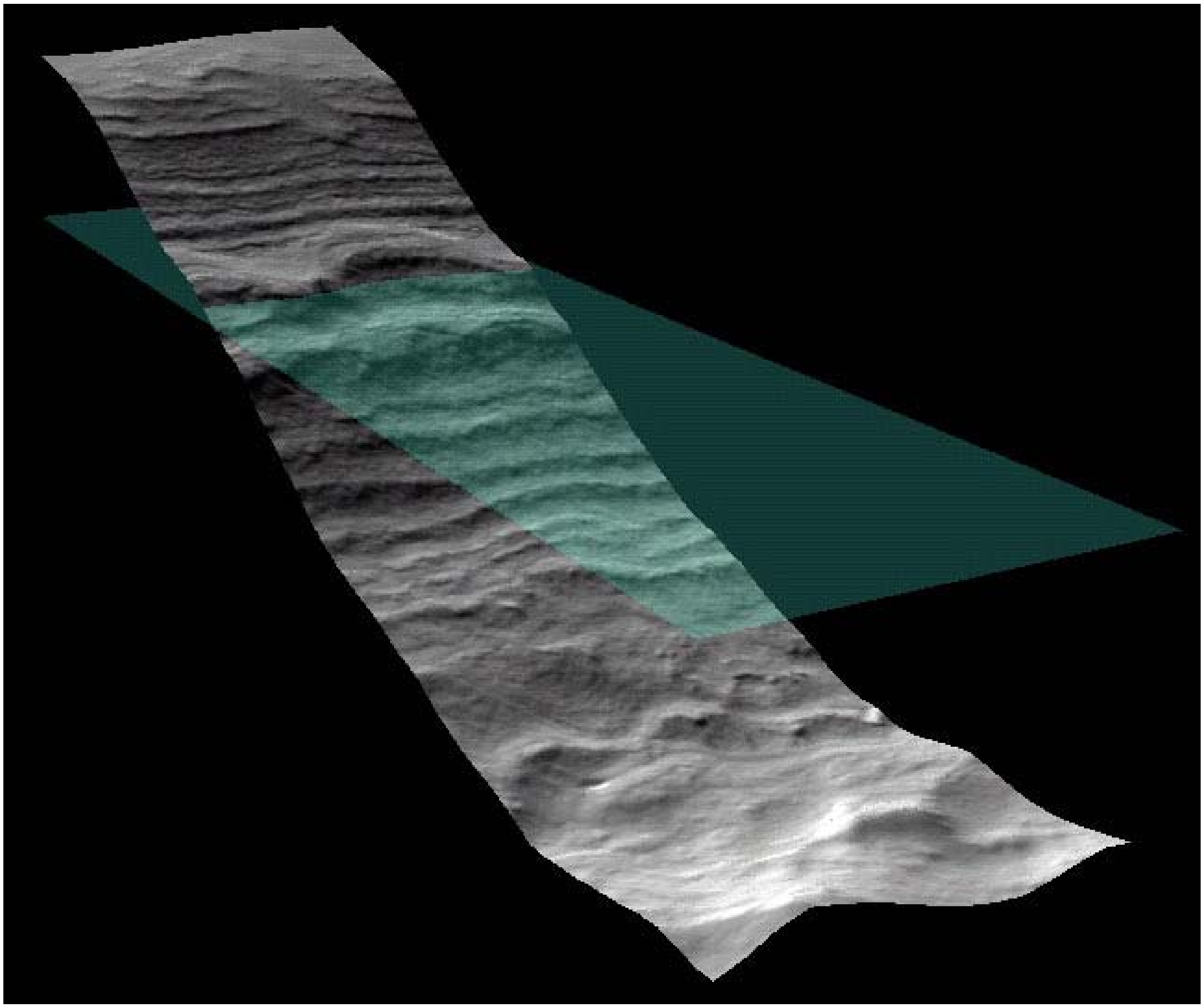

Figure 2. Oblique view of digital elevation model derived from MOC narrow angle image m0905983 (2.7 m/pixel) of south polar layered deposits. Green plane is horizontal reference surface. Note that bedding is not everywhere horizontal, perhaps due to faulting or flow of originally flat-lying layers.

THE SOUTH POLAR RESIDUAL CAP OF MARS:LAYERS, EROSION, AND STRATIGRAPHY.

P. C. Thomas[1] [1]Center for Radiophysics and Space Research, Cornell University, Ithaca NY, 14853.

The south polar residual cap (sprc) of Mars is a group of thin layers degraded into unique topography resting on the flatter portions of the main polar layered deposits. This is a summary of the characteristics of these layers and their degredation that impacts the interpretation of the history of the martian polar environment..

Residual cap layers: There are two primary sets of depositional units in the sprc: 1) An older unit, approximately 10 m in thickness with four or five included layers, widely distributed over the sprc, and expressed as mesas or broad surfaces cut by a variety of circular to linear depressions, and commonly having polygonal troughs on the uppermost surface. Shadow and MOLA measurements show these layers are ~2 m in thickness. The layers can be exposed in scarps over 30° in slope, but commonly the lower portions of exposed layers are covered by debris with much lower slopes, and also commonly display a patterned surface that can be confused with layering.

2) One or more younger units, approximately 1-2 m thick, that have superposed and filled depressions formed in the older unit, and also formed in local discrete deposits. This unit also has a wide variety of depression types.

Both units show scarp retreat of up to a few m over one Martian year [1].

Erosion and other modification forms: The sprc topography has unique erosional topography [2,3]. Large circular depressions 300 –1000+ m across that cut two to four (perhaps 5) of the layers occur across the sprc. Linear depressions, asymmetric in cross section, usually cutting two-three layers, occur in the central portion of the sprc. Their trends suggest some underlying structural control, while the cross sectional asymmetry may be related to insolation asymmetry. Curled depressions grade into other forms, and show a preferred opening direction toward the north. Other depressions can be irregularly-shaped, and some areas have been largely stripped of the sprc layers by merging depressions. Moat-like depressions occur within some nearly circular forms as well as bounding a variety of mesas and other remnant topography. Moats within depressions show two distinct widths: ~20 m and ~70 m. The latter is indistinguishable from moat widths around mesas and other remnants.

Development of the depressions and deposits: Initiation of many of these forms appears to involve sag and collapse (Fig. 1a,d). Backwasting of the steeper slopes then enlarges the depressions. Changes between 1999 and 2001 indicate some backwasting of the forms of order 1-4 m/ Mars year [1], with a few instances over 5 m. Development sequences of curled depressions can be found, and examples of enlargement almost entirely by collapse are also found (Fig. 1a,d). The sag and collapse features may explain the development of "escher" terrain, whereby an upper surface appears contiguous between different cycles of erosion (Fig. 1d,e).

Most interesting is the development of inverted relief (Fig. 1f-h). The large, scalloped mesas have in some instances collapsed below the level of embaying deposits that in most other instances are lower than the mesa remnants. Different stages of this development can be found in the sprc. The preferred collapse of some materials suggests significant variations in the susceptibility to sublimation of these deposits.

Thin layers preferentially develop pits and other depressions over underlying topography, and on some upper convex slopes. These pits, "peels", and moats indicate modification of overlying deposits by exposure of relief or a critical layer thickness.

Non-uniform deposition is also found in some tongues of material several m in depth and a few hundred m long in restricted areas of the sprc. These appear to be part of the later deposits.

Interpretations: Several different cycles/changes in polar depositional and sublimational regime are indicated:

1). Change from main polar layered deposits to deposition of the sprc: H_20 rich deposits to CO_2 rich ones.

2) Cycles producing layering within the 10 m stack, about 4-5 cycles. Some differences in physical characteristics/ composition.

3) Significant erosion of the deposits in the form of merging depressions and sag and collapse modification.

4) Before or during the subsequent steps, development of polygonal troughs in much of the surface of the thick deposit.

5) Deposition of one or two, ~1- 2 m layers in the erosional topography of the thick deposits, and/or smoothing of surface of a lag deposit left by collapse and backwasting of the layers.

6) Renewed sublimation and collapse of both deposits. Included in this step is the scattered development of inverted relief. This activity may continue at present.

The evident variety of layer types, thicknesses, and cycles of deposition and erosion show there are several combinations of composition and/or texture within these deposits. The sag and collapse suggest a possible role for either absorption of insolation at depth, or a geothermal role in sublimation or other modification of the layers. Loss of substantial porosity might be a part of the collapse sequence. The inverted relief and the other forms surrounding mesa remnants indicate at least one major change in the thermal environment of the layers since major sublimation loss began.

References:

[1] Malin, M. C., M. A. Caplinger, and S. D. Davis (2001). *Science, 294*, 2146-2148. [2] Thomas, P. C. et al. (2000). *Nature 404*, 161-164. [3] Byrne, S., and A. P. Ingersoll (2003). *Science 299*, 1051-1053.

Acknowledgements: Help was provided by Mike Malin, Ken Edgett, Scott Davis, Bruce Cantor, Brian Carcich, Rob Sullivan, Karla Consroe, and Lisa Wei.,.

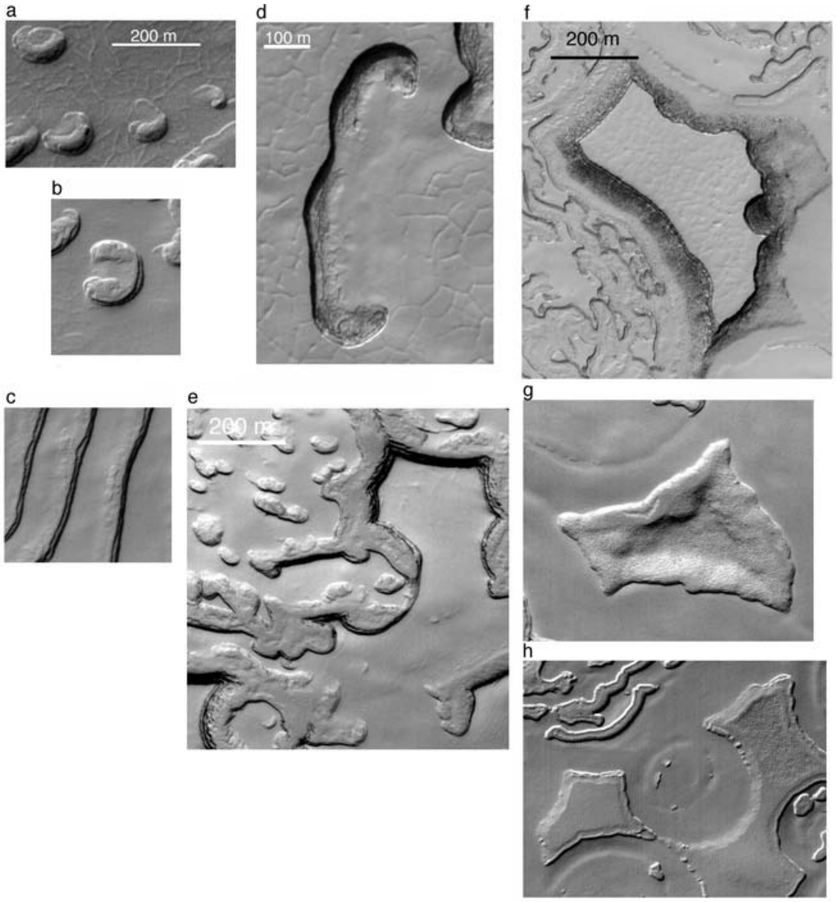

Figure 1a. Sequence of development of curl depressions by collapse and fracture. Illumination is from lower right. b. Curl depression showing ramp from upper surface. Illumination is from lower right. c. Fingerprint depressions; steep on right side, gentle slope on left. Sun is from lower right. Compare gentle slope on left to ramp in Fig. 1b. d. Depression at margin of sag in upper surface. Compare Fig. 1b. Illumination is from upper left. e. Remnant of several layers, near upper right, which tapers to feather edge at lower right. Possible later deposit embays the scalloped margin of the tapering set of layers. Illumination is from lower right. f. Typical remnant of layers, about 10 m above surroundings. Edges are patterned debris. g. Patterned debris from near complete collapse of material such as that in 1f, with overlying deposit (or, less likely, a different form of collapse material). Illumination is from lower right. h. Inverted relief. The scalloped topography of mesas (such as 1f.) has collapsed to a level lower than occupied by embaying materials (note circular feature in middle is high relative to surroundings, illumination is from lower right).

Climactic history from south polar residual cap geomorphology.

S. Byrne[1], A.P. Ingersoll[1], A.V. Pathare[1] and F.S. Jiron[1], [1]Division of Geological and Planetary Sciences, California Institute of Technology, Mail-stop 150-21, 1200 East California Blvd., Pasadena, CA 91125, USA. **shane@gps.caltech.edu**, **api@gps.caltech.edu**, **avp@gps.caltech.edu**, **franklin@its.caltech.edu**

Introduction: The southern residual CO_2 cap is a small (88,000 km^2) high-albedo feature which sits atop the much thicker and more extensive southern layered deposits. It persists throughout the year in contrast to the thinner seasonal CO_2 frost which appears and disappears each year. The solid CO_2 which lasts throughout the year both controls circulation patterns regionally and buffers the atmospheric pressure globally. In turn this residual CO_2 deposit is affected by changes in environmental conditions wrought by external forces such as dust storm activity.

This solid CO_2 reservoir has been theorized and observed for decades [1, 2]. Mars Global Surveyor data have revealed this CO_2 residual deposit to contain a rich variety of geomorphic features [3]. One of the most ubiquitous classes of features on the residual cap are the flat-floored quasi-circular pits with steep walls (see Fig. 1), dubbed Swiss-cheese features.

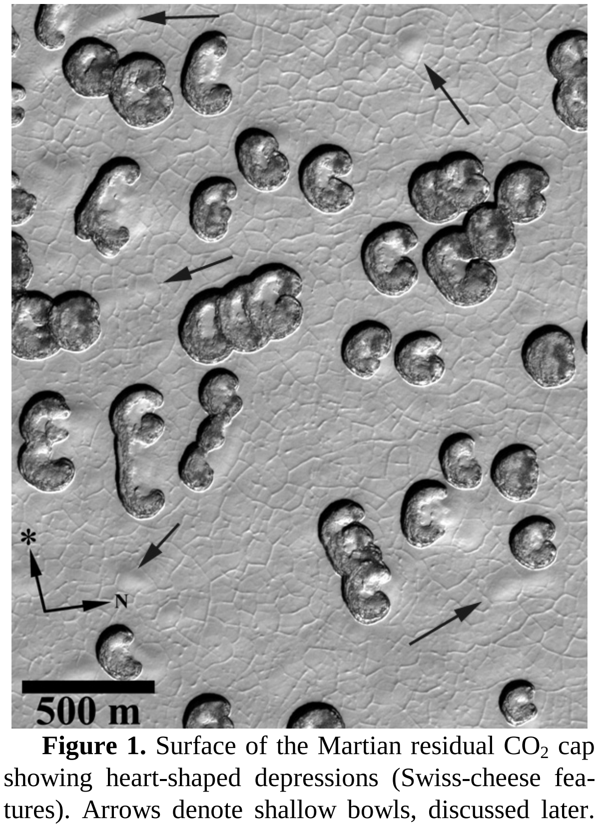

Figure 1. Surface of the Martian residual CO_2 cap showing heart-shaped depressions (Swiss-cheese features). Arrows denote shallow bowls, discussed later. Sub-frame of MOC narrow angle image E13/00663, 87° S, 352° E, L_s 323° (late southern summer), bottom arrows denote direction to sun and north.

Feature description: Swiss-cheese features are characterized by flat floors and steep walls. Features in the region shown in figure 1 and discussed in the next section have a definite symmetry axis found to point in the north-south direction (7). Features in other parts of the cap commonly posses a raised central island in their center surrounded by a moat.

Late in the southern summer when the seasonal covering of CO_2 frost has been removed the walls can be seen to be darker than the surrounding flat upper surfaces.

No changes in shape or size were observed in these features over timescales of a single season (3, 5) but *Malin et al.* (6) observed, using images separated by one Martian year, that the walls of these depressions are expanding laterally at rates of 1-3 m/yr. The rapidity of this expansion is only possible in a medium as volatile as CO_2 ice. *Byrne and Ingersoll* (4) modeled the evolution and growth of these depressions as a hole in a layer of CO_2 ice underlain by water ice and matched their observed expansion rates and morphologic properties, including the flat floors and steep walls.

Swiss-cheese features in local regions all exhibit the same depth, *i.e.*, they all penetrate to the base of the CO_2 deposit, their downward expansion being halted by the involatile nature of the water-ice substrate (4). Different areas on the residual cap exhibit differing thicknesses of the overlying CO_2 slab. The thickest CO_2 deposits appear to be 8-10 meters; however most of the rest of the cap has a much thinner covering. In features which possesses moats and raised central islands it is the moat which penetrates to the underlying water ice layer (7). Modeling results indicate however that the thickness of the overlying CO_2 slab does not affect the retreat rates of the walls.

Environmental history from Swiss-cheese feature populations: The fast rate of wall retreat observed (6) and modeled (4) combined with the small sizes of the depressions indicate that all Swiss-cheese features visible today were created recently (7). Our modeling results indicate that walls should retreat at constant rates once the initial formation phase is over.

In previous work we selected a study region within the residual cap and measured the sizes and orientations of all Swiss-cheese features that it contained (see figure 2). The size distribution is quite narrow indicating that the measured population has initiated over a very short period of time. We estimate this formation period to have occurred 43-217 Martian years ago. The large spread in age is due to the large spread in modeled wall retreat rates. Values ranging from 0.5-2.5 m/yr are possible with different subsurface albedo conditions (4).

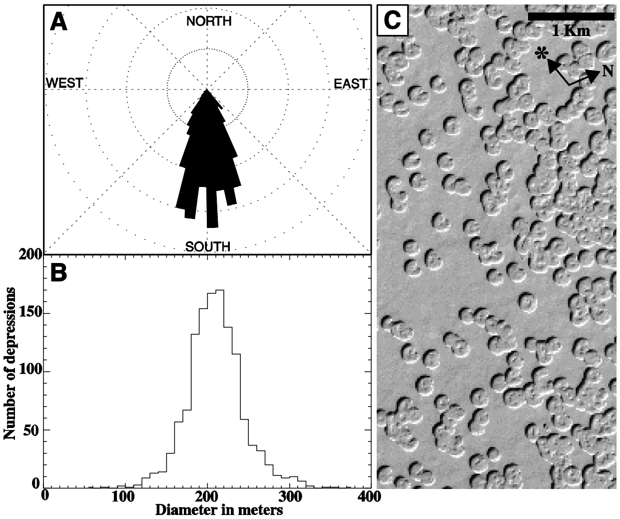

Figure 2. Taken from (7). **A)** Rose diagram of Swiss-cheese feature orientations. Azimuth refers to the direction from the cusp to the opposite wall, through the center of the depression. The total number of features measured was 370, the mean azimuth was within 0.2° of south and the standard deviation was ~17°. Concentric circles indicate number in increments of 10. **B)** Histogram of sizes of identifiable Swiss-cheese features. Diameter here refers to the longest axis for non-circular features. The total number of features measured is 1263, the mean size was 217m and the standard deviation was ~35m. **C)** Many Swiss-cheese features destroying the upper 8m thick layer in a sample view of the study area. Sub-frame of MOC narrow angle image M07/04167, taken at 86.8° S, 355° E, and L_s 211°.

Some change in environmental conditions started this particular population of features growing. Unfortunately we have only begun to observe Mars in detail over the past few decades so understanding what the nature of this event may have been is difficult.

The shallow bowls that are indicated by arrows on figure 1 may be a new generation of Swiss-cheese features. If this is the case we would expect from our modeling that these features would be less than 30 Martian years old. One significant event in Martian history that may have been responsible for their genesis is the 1971 global dust storm. This would lead to increased erosion of the residual cap, but it is unclear why that would initiate the growth of isolated depressions. If the number density of features is an indication of the severity of the event that initiated them, then the event which initiated the main population discussed above and in figure 2 must have been much more severe than this dust storm.

Work to be presented: There are several avenues of research that we are perusing and which will be presented.

- We will report on investigations into the overall mass budget of the CO_2 residual cap. If the Swiss-cheese feature walls are retreating and the mass is not being recondensed elsewhere on the cap then the cap itself will disappear within a few Martian centuries. It seems unlikely that we are observing Mars at such a special time in its history.
- A large range of expansion rates is possible depending on the subsurface albedo profile (4, 7). This is a major obstacle in using our modeling results to date observed Swiss-cheese populations. We will attempt to measure the subsurface albedo profile by examining Mars Orbiter Camera (MOC) images of exposures in the walls of the Swiss-cheese features.
- We have already modeled the initial growth of Swiss-cheese features. However, we always initiated our modeled depressions from pre-existing small surface features. We will report on more detailed investigations into the genesis of Swiss-cheese populations and the possible link to climactic events such as the 1971 dust storm.
- We will continue to catalogue new population statistics for different regions in the residual cap. Each distinct new Swiss-cheese population that we can identify will give us information on previous environmental events that may have occurred.

Investigations into Swiss-cheese features have the potential to describe the last millennia of Martian polar history. It will provide a link from present conditions to longer term variations in Martian climate (due to changing orbital elements) which are perhaps recorded in the layered deposits.

References: [1] Leighton, R. B., and B. C. Murray, *Science* (1966) *153*, 136-144. [2] Kieffer, H. H. (1976) *JGR*, *84*, 8263-8288. [3] Thomas P. C. et al. (2000) *Nature*, *404*, 161-164. [4] Byrne, S., and A. P. Ingersoll (2003) *Science*, *299*, 1051-1053. [5] Malin, M. C., and K. S. Edgett (2001) *JGR*, *106*, 23429-23570. [6] Malin, M. C. et al. (2001) *Science*, *294*, 2146-2148. [7] Byrne, S., and A. P. Ingersoll (2003) *GRL, 30(13)*.